

# RHEED oscillations in spinel ferrite epitaxial films grown by conventional planar magnetron sputtering

著者	Ojima T., Tainosho T., Sharmin S., Yanagihara H.
journal or publication title	AIP Advances
volume	8
number	4
page range	045106
year	2018-04
権利	(C) 2018 Author(s). All article content, except where otherwise noted, is licensed under a Creative Commons Attribution (CC BY) license ( <a href="http://creativecommons.org/licenses/by/4.0/">http://creativecommons.org/licenses/by/4.0/</a> ). <a href="https://doi.org/10.1063/1.5012133">https://doi.org/10.1063/1.5012133</a>
URL	<a href="http://hdl.handle.net/2241/00153079">http://hdl.handle.net/2241/00153079</a>

doi: 10.1063/1.5012133

## RHEED oscillations in spinel ferrite epitaxial films grown by conventional planar magnetron sputtering

T. Ojima, T. Tainosho, S. Sharmin, and H. Yanagihara

Citation: *AIP Advances* **8**, 045106 (2018); doi: 10.1063/1.5012133

View online: <https://doi.org/10.1063/1.5012133>

View Table of Contents: <http://aip.scitation.org/toc/adv/8/4>

Published by the [American Institute of Physics](#)

---

### Articles you may be interested in

[Modification of YNbO<sub>4</sub> and YNbTiO<sub>6</sub> photoluminescence by nitrogen doping](#)

*AIP Advances* **8**, 045107 (2018); 10.1063/1.5012071

[Flexible and stackable terahertz metamaterials via silver-nanoparticle inkjet printing](#)

*AIP Advances* **8**, 045104 (2018); 10.1063/1.5006867

[Study on the mechanism of a manganese-based catalyst for catalytic NO<sub>x</sub> flue gas denitration](#)

*AIP Advances* **8**, 045004 (2018); 10.1063/1.4989431

[Synthesis science of SrRuO<sub>3</sub> and CaRuO<sub>3</sub> epitaxial films with high residual resistivity ratios](#)

*APL Materials* **6**, 046101 (2018); 10.1063/1.5023477

[Ferroelectric or non-ferroelectric: Why so many materials exhibit “ferroelectricity” on the nanoscale](#)

*Applied Physics Reviews* **4**, 021302 (2017); 10.1063/1.4979015

[A contact-force regulated photoplethysmography \(PPG\) platform](#)

*AIP Advances* **8**, 045210 (2018); 10.1063/1.5020914

---

**AIP** | Conference Proceedings

Get **30% off** all  
print proceedings!

Enter Promotion Code **PDF30** at checkout



## RHEED oscillations in spinel ferrite epitaxial films grown by conventional planar magnetron sputtering

T. Ojima, T. Tainosho, S. Sharmin, and H. Yanagihara<sup>a</sup>

*Institute of Applied Physics, University of Tsukuba, Tsukuba 305-8573, Japan*

(Received 6 November 2017; accepted 23 March 2018; published online 6 April 2018)

Real-time *in situ* reflection high energy electron diffraction (RHEED) observations of  $\text{Fe}_3\text{O}_4$ ,  $\gamma\text{-Fe}_2\text{O}_3$ , and  $(\text{Co,Fe})_3\text{O}_4$  films on  $\text{MgO}(001)$  substrates grown by a conventional planar magnetron sputtering was studied. The change in periodical intensity of the specular reflection spot in the RHEED images of three different spinel ferrite compounds grown by two different sputtering systems was examined. The oscillation period was found to correspond to the  $1/4$  unit cell of each spinel ferrite, similar to that observed in molecular beam epitaxy (MBE) and pulsed laser deposition (PLD) experiments. This suggests that the layer-by-layer growth of spinel ferrite (001) films is general in most physical vapor deposition (PVD) processes. The surfaces of the films were as flat as the surface of the substrate, consistent with the observed layer-by-layer growth process. The observed RHEED oscillation indicates that even a conventional sputtering method can be used to control film thickness during atomic layer depositions. © 2018 Author(s). All article content, except where otherwise noted, is licensed under a Creative Commons Attribution (CC BY) license (<http://creativecommons.org/licenses/by/4.0/>). <https://doi.org/10.1063/1.5012133>

Among various physical vapor deposition (PVD) techniques, magnetron sputtering is probably the most conventional and has been widely used from laboratory fundamental research to mass industrial production. The magnetron sputtering process for thin film growth possesses significant advantages compared to other PVD techniques, such as high throughput rate, process stability, reproducibility, and convenience for growing films of alloys and metals with high melting point.<sup>1</sup> However, because sputtering is a relatively high-energy plasma assisted process, the film quality may be much different or worse than that grown by other PVD processes such as molecular beam epitaxy (MBE) and pulsed laser deposition (PLD). Nevertheless, previous reports on the epitaxial film growth of tin-oxide<sup>2</sup> and high- $T_c$  superconductors<sup>3-5</sup> have suggested that layer-by-layer growth can be realized even during conventional reactive sputtering processes. Unfortunately, because of a lack of *in situ* precise control/monitoring technique of conventional magnetron sputtering, such methods have not been considered suitable for growing films with well-controlled atomic scale thickness.

To monitor both surface conditions and the crystal structure during the film growth process, a reflection high energy electron diffraction (RHEED) measurement is one of the simplest *in situ* techniques. In fact, RHEED is the most common monitoring technique for MBE and PLD systems. *In situ* RHEED observations have also been reported for particular sputtering methods such as 90-degree-off sputtering<sup>6</sup> and ion-beam sputtering.<sup>7</sup>

The epitaxial growth process is classified into three modes; island growth (Volmer-Weber mode), layer-by-layer growth (Frank-van der Merwe mode) and layer-plus-island growth (Stranski-Krastanov mode). For the layer-by-layer film growth mode, the intensity of the specular spot reflection in the RHEED images oscillates with a period corresponding to the growth time of the monolayer/molecular-layer thickness. Besides providing an understanding of the growth mode, real-time *in situ* RHEED observation enables precise controls and/or monitoring of real-time determination of film

<sup>a</sup>Electronic mail: [yanagiha@bk.tsukuba.ac.jp](mailto:yanagiha@bk.tsukuba.ac.jp)

thickness,<sup>8</sup> composition,<sup>9</sup> atomically flat surface/interface,<sup>10</sup> superlattice structures,<sup>11</sup> emergence of misfit dislocations<sup>12</sup> and so on.

Although conventional planar-type magnetron sputtering is widely employed in industries as well as in laboratories, *in situ* RHEED experiments have not been carried out to our knowledge. Unlike a 90-degree-off sputtering technique, the stray magnetic field that the *e*-beam experiences in the RHEED system is symmetric even for a single cathode system. In addition, the design of magnetron sputtering cathodes has been improved to concentrate the magnetic field closer to the target surfaces enabling long-throw-sputtering,<sup>13</sup> so that the stray field around the *e*-beam path can be expected to be sufficiently weak. Nowadays *e*-guns for RHEED with a differential pumping system is quite common. Therefore, real-time *in situ* RHEED monitoring during the sputtering process can be realized and is expected to give details of the thin film growth process,<sup>14</sup> similar to the MBE and PLD cases. In this letter, we report that *in situ* RHEED intensity oscillations occur during the film growth processes of Fe<sub>3</sub>O<sub>4</sub> (001),  $\gamma$ -Fe<sub>2</sub>O<sub>3</sub>(001), and Co<sub>0.75</sub>Fe<sub>2.25</sub>O<sub>4</sub>(001)(CFO) films grown on MgO(001) in a conventional planar rf-sputtering system. Our observation suggests that layer-by-layer growth can be generally observed in PVD processes and is quite a common phenomenon.

Three different spinel ferrite films Fe<sub>3</sub>O<sub>4</sub>,  $\gamma$ -Fe<sub>2</sub>O<sub>3</sub>, and CFO were grown by planar reactive magnetron sputtering, introducing oxygen as a reactive gas with a metal or alloy target. The details of the growth conditions can be found in Refs. 15 and 16. All the films were grown by rf magnetron sputtering on a cleaved MgO(001) single crystal as the substrate. We examined two different sputtering systems equipped with 2-inch cathodes. (001) and CFO(001) films were deposited by Eiko's sputtering system of ES-250MB.  $\gamma$ -Fe<sub>2</sub>O<sub>3</sub>(001) films were independently deposited by two systems of ULVAC's MPS-6000 and ES-250MB. Hereafter, we refer to samples with the name of the compound followed with (U) or (E), depending on the sputtering system. For example,  $\gamma$ -Fe<sub>2</sub>O<sub>3</sub>(U) stands for a  $\gamma$ -Fe<sub>2</sub>O<sub>3</sub> film grown by the ULVAC system.

Process temperature for all spinel ferrite films was kept at 300°C and a typical distance between the target and substrate was adjusted to be between 18 and 20 cm so that the RHEED image could be most clearly obtained. For growing Fe<sub>3</sub>O<sub>4</sub> and  $\gamma$ -Fe<sub>2</sub>O<sub>3</sub> films, we used Fe target and for CFO, we used CoFe(1:3) alloy target. Process pressure in the chamber was maintained at approximately  $\sim 10^{-1}$  Pa. During sputtering deposition, RHEED images were recorded with the incident *e*-beam parallel to the MgO[010] azimuth. The acceleration voltage of the *e*-beam was 30 kV and the emission current was between 56-60  $\mu$ A. It is to be noted that our RHEED devices had a differential pumping system. The RHEED images during deposition were recorded as moving images of 10 frames/second and the intensity change of the specular reflection of the RHEED image was investigated with respect to process time. After film growth, the film thickness *D* was determined by X-ray reflectivity (XRR) with a conventional X-ray diffractometer and the surface condition was measured with an atomic force microscope (AFM). The details of the equipment used are shown in Table I.

RHEED images of (a) MgO(001) substrate, (b)  $\gamma$ -Fe<sub>2</sub>O<sub>3</sub>(001)(U), (c) Fe<sub>3</sub>O<sub>4</sub>(001)(E), (d)  $\gamma$ -Fe<sub>2</sub>O<sub>3</sub>(001)(E), and (e) CFO(001)(E) are shown in Fig. 1. Clear streaks and Kikuchi lines are observed in all images, suggesting that the films are epitaxially grown with sufficiently flat surfaces and high crystallinities. RHEED images shown in Fig. 1(b)–(e) are similar to previously reported RHEED patterns for spinel ferrite (001) films.<sup>15,17,18</sup> Moreover, additional streaks can

TABLE I. Details of the equipment/devices.

Equipment/devices	Supplier and Product Names/Specifications
Camera	Basler acA640-750 $\mu$ m/CMOS(VGA), interface: USB3.0
Lens	Basler Lens C125-0418-5M/focal length =4.0mm, iris = F1.8-22.0
PC	CPU: Intel Core i5-6200U (2.3-2.8GHz), memory: 4GB
Sputtering system	ULVAC MB03-1030/6 x 2-inch cathodes, rf and dc sputtering
RHEED gun	Eiko ES-250MB/2-inch cathode, rf sputtering R-DEC RDA-001GD with differential pumping system

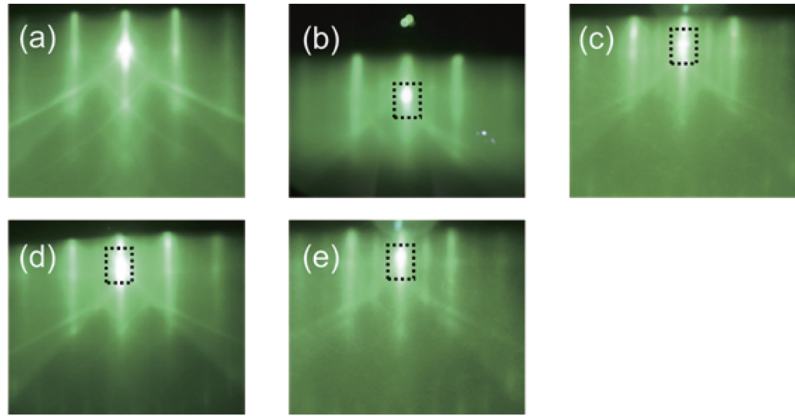


FIG. 1. RHEED images of (a) MgO(001) substrate, (b)  $\gamma$ -Fe<sub>2</sub>O<sub>3</sub> deposited by ULVAC MPS-6000, (c) Fe<sub>3</sub>O<sub>4</sub>, (d)  $\gamma$ -Fe<sub>2</sub>O<sub>3</sub>, and (e) CFO deposited by Eiko ES-250MB. Specular reflection spots of the electron beam are indicated by rectangular areas shown by broken lines.

be seen in Fig. 1(b) of (001), suggesting the film of (001) has a reconstructed surface spinel structure.<sup>18</sup>

In order to determine film thickness, we performed XRR experiments. Figure 2 shows the XRR patterns of (a)  $\gamma$ -Fe<sub>2</sub>O<sub>3</sub>(U), (b) Fe<sub>3</sub>O<sub>4</sub>(E), (c)  $\gamma$ -Fe<sub>2</sub>O<sub>3</sub>(E), and (d) CFO(E). All films exhibit clear oscillations in the XRR patterns. The film thickness  $D$  can be estimated from the XRR oscillation as a function of scattering angle  $\theta$ , through the relation  $2D\sin\theta = n\lambda$ . Here,  $\lambda$  indicates the wavelength of the X-ray source and  $n$  is an integer. The determined film thickness of all the films are listed in Table II.

The intensity change in the specular reflection spot of the RHEED image during deposition of (a)  $\gamma$ -Fe<sub>2</sub>O<sub>3</sub>(U) and (b) Fe<sub>3</sub>O<sub>4</sub>(E), (c)  $\gamma$ -Fe<sub>2</sub>O<sub>3</sub>(E), (d) CFO(E) is shown in Fig. 3. No matter which sputtering system was used, clear RHEED intensity oscillations are observed for all film growth processes, suggesting that layer-by-layer growth occurs. In the case of  $\gamma$ -Fe<sub>2</sub>O<sub>3</sub>(U) film, for example, the average period of intensity change was 27.9 sec. On the other hand, the growth rate can be estimated from the total thickness  $D$  divided by the process time  $t_P$ , which is  $D/t_P = 0.0756$  Å/sec.

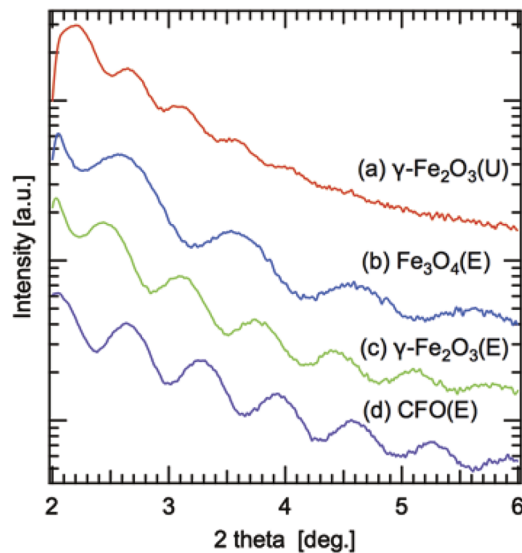


FIG. 2. X-ray reflectivity patterns of (a)  $\gamma$ -Fe<sub>2</sub>O<sub>3</sub> deposited by ULVAC MPS-6000, (b) Fe<sub>3</sub>O<sub>4</sub>, (c)  $\gamma$ -Fe<sub>2</sub>O<sub>3</sub> and (d) CFO deposited by Eiko ES-250MB.

TABLE II. Oscillation periods and thicknesses of the grown thin films.

Sample	Lattice constant (bulk) $a$ [Å]	Refs.	Process time $t_P$ [sec]	Film thickness $D$ [Å]	Period of oscillation $\bar{T}$ [sec]	Growth rate $D/t_P$ [Å/s]	$\bar{T}D/t_P$ [Å]
$\gamma$ -Fe <sub>2</sub> O <sub>3</sub> (U)	$2.088 \times 4 = 8.352$	19	2400.0	181.4	27.9	0.0756	2.11
Fe <sub>3</sub> O <sub>4</sub> (E)	$2.099 \times 4 = 8.395$	20	300.0	87.2	7.4	0.291	2.15
$\gamma$ -Fe <sub>2</sub> O <sub>3</sub> (E)	$2.088 \times 4 = 8.352$	19	2400.0	134.6	37.7	0.0561	2.11
CFO(E)	$2.095 \times 4 = 8.380$	21	600.0	135.8	9.8	0.226	2.21

Therefore, the average period of intensity oscillation can be calculated to be 2.11 Å. This thickness corresponds to the  $\frac{1}{4}$  unit cell of  $\gamma$ -Fe<sub>2</sub>O<sub>3</sub> within experimental error. RHEED oscillations with thickness corresponding to  $\frac{1}{4}$  unit cell of spinel ferrite has been widely observed in MBE<sup>18</sup> and PLD<sup>17</sup> for Fe<sub>3</sub>O<sub>4</sub>(001) film growth. Note that the thickness of the  $\frac{1}{4}$  unit cell of spinel ferrites accords to a thickness of one molecular unit of spinel structure along [001] stacking. Moreover, the film growth processes for other compounds of Fe<sub>3</sub>O<sub>4</sub>(E),  $\gamma$ -Fe<sub>2</sub>O<sub>3</sub>(E), and CFO(E) also exhibit clear RHEED intensity oscillations with thickness corresponding to the  $\frac{1}{4}$  unit cell of the lattice constant,<sup>19–21</sup> as summarized in Table II. Therefore, the growth mode of these spinel ferrite thin films by planar sputtering is the sequential layer-by-layer assembly similar to that by other PVD techniques such as PLD and MBE.

AFM images of (a) and (b) MgO(001) substrate and (b) CFO(E) are shown in Fig. 4. Since the MgO(001) substrate surface was cleaved, the terraced area is supposed to be atomically flat. In fact, only two steps with the height less than 1 nm were found in the wide-area measurement of MgO(001) as shown in Fig. 4(a). There was no significant change in the root mean square roughness ( $R_{\text{rms}}$ ) of the substrate ( $R_{\text{rms}}^{\text{subst}} = 6.38 \times 10^{-2}$  nm) and that of the film ( $R_{\text{rms}}^{\text{CFO}} = 6.98 \times 10^{-2}$  nm), consistent with the observed layer-by-layer growth in the CFO(E) film. 's of the other films are comparable to  $R_{\text{rms}}^{\text{CFO}}$ .

Figure 5 exhibits the Fourier analysis of 2048 data points of the RHEED oscillation for the Fe<sub>3</sub>O<sub>4</sub>(E) film. We used a fast Fourier transformation (FFT) package with Hamming window. One can clearly see peaks at frequencies corresponding to the  $\frac{1}{4}$  unit cell and its integers. As mentioned above, the oscillation period of the  $\frac{1}{4}$  unit cell indicates a molecular layer of a spinel structure stacked along the [001] direction. Although there is no peak at the frequency associated with the lattice constant, a clear peak at the frequency corresponding to the thickness of

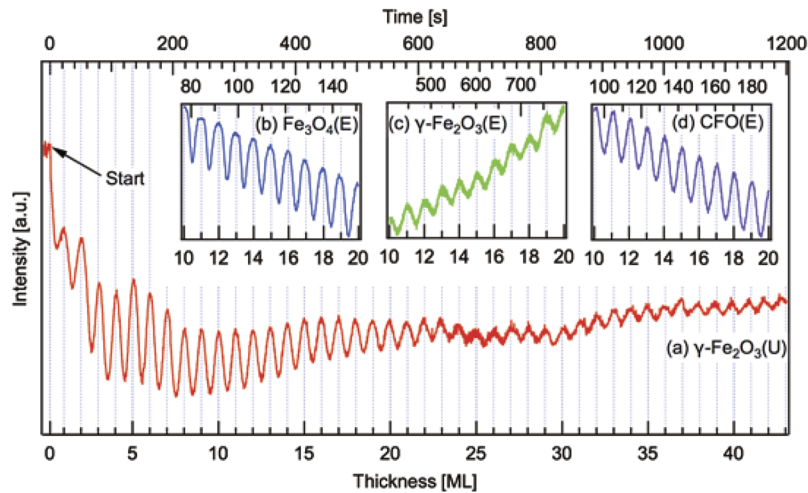


FIG. 3. Temporal variations of specular spot intensity of the RHEED images of (a)  $\gamma$ -Fe<sub>2</sub>O<sub>3</sub> deposited by ULVAC MPS-6000, (b) Fe<sub>3</sub>O<sub>4</sub>, (c)  $\gamma$ -Fe<sub>2</sub>O<sub>3</sub>, and (d) CFO deposited by Eiko ES-250MB. Bottom axes are ticked with a unit of monolayer (ML), while the top axes indicate in second.



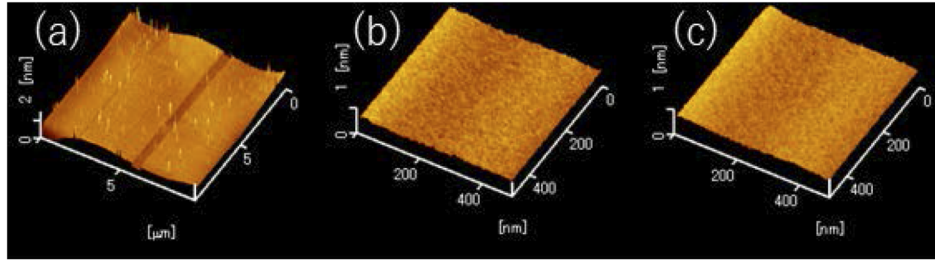


FIG. 4. AFM images of  $10\mu\text{m}^2$  scan of (a) MgO(001) substrate and  $0.5\mu\text{m}^2$  scans of (b) MgO(001) substrate and (c) CFO(001) film.

the  $5/2$  unit cell is found only for  $\text{Fe}_3\text{O}_4(\text{E})$  but not in the other ferrite films. This may suggest the existence of some superstructure or reconstruction in the  $\text{Fe}_3\text{O}_4(001)$  films along the growth direction.

In summary, we tested real-time *in situ* RHEED observation of the film growth processes of  $\text{Fe}_3\text{O}_4$ ,  $\gamma\text{-Fe}_2\text{O}_3$ , CFO on MgO(001) substrates by conventional planar magnetron sputtering. We observed sharp streaks and clear Kikuchi lines in the RHEED pattern measured with a differential pumping system during the sputtering processes. The periodic intensity change of the specular reflection spot of the RHEED images was confirmed and the average oscillation period corresponded to the  $1/4$  unit cell of each spinel ferrite, identical to that observed in MBE and PLD experiments. Our results suggest that layer-by-layer growth of spinel ferrite (001) films is general in most PVD processes. The fact that the surface of the film is as flat as the surface of the substrate is consistent with the layer-by-layer growth process. The observed RHEED intensity oscillation phenomena indicate that atomically precise thickness control is possible even with a conventional planar sputtering method.

This study was supported in part by the Japan Science and Technology Agents (JST) under the collaborative research program, based on industrial demand, titled “High Performance Magnets: towards innovative development of next generation magnets”, in part by the ImPACT Program of the Council for Science, Technology and Innovation (Cabinet Office, Government of Japan) and in part by JSPS KAKENHI under Grant JP15K13355 and 15H03966.

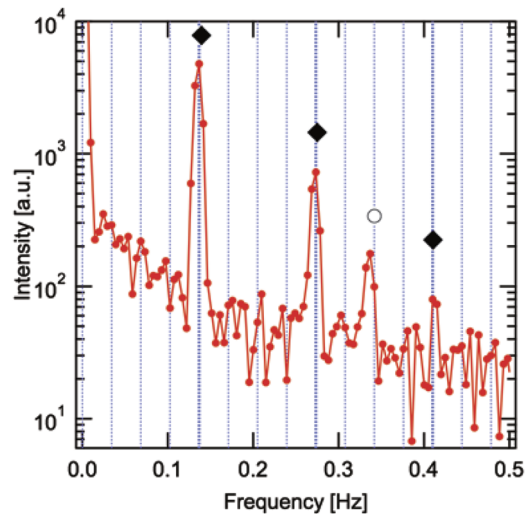


FIG. 5. FFT spectra of the specular spot intensity of the RHEED images of  $\text{Fe}_3\text{O}_4$  (Fig. 2(b)). Diamonds indicate the fundamental and the integral multiple frequencies corresponding to the inverse of the growth time for the  $1/4$  unit cell. Open circle corresponds to the  $5/2$  unit cell.

- <sup>1</sup> X. Sun, E. Kolawa, J. S. Chen, J. S. Reid, and M. A. Nicolet, *Thin Solid Films* **236**, 347 (1993).
- <sup>2</sup> R. E. Cavicchi, S. Semancik, M. D. Antonik, and R. J. Lad, *Appl. Phys. Lett.* **61**, 1921 (1992).
- <sup>3</sup> K.-Y. Yang, M. S. Dilorio, S. Yosizumi, M. A. Maung, J. Zhang, P. K. Tsai, and M. B. Maple, *Appl. Phys. Lett.* **61**, 2826 (1992).
- <sup>4</sup> M. Hawley, I. D. Raistrick, J. G. Beery, and R. J. Houlton, *Science* **251**, 1587 (1991).
- <sup>5</sup> C. Gerber, D. Anselmetti, J. G. Bednorz, J. Mannhart, and D. G. Schlom, *Nature* **350**, 279 (1991).
- <sup>6</sup> J. P. Podkaminer, J. J. Patzner, B. A. Davidson, and C. B. Eom, *APL Mater.* **4**, 86111 (2016).
- <sup>7</sup> S. Nishizawa, T. Tsurumi, H. Hyodo, Y. Ishibashi, N. Ohashi, M. Yamane, and O. Fukunaga, *Thin Solid Films* **302**, 133 (1997).
- <sup>8</sup> A. Gupta, M. Y. Chern, and B. W. Hussey, *Phys. C Supercond. Its Appl.* **209**, 175 (1993).
- <sup>9</sup> J. H. Haeni, C. D. Theis, and D. G. Schlom, *J. Electroceramics* **4**, 385 (2000).
- <sup>10</sup> H. Sakaki, M. Tanaka, and J. Yoshino, *Jpn. J. Appl. Phys.* **24**, L417 (1985).
- <sup>11</sup> T. Sakamoto, H. Funabashi, K. Ohta, T. Nakagawa, N. J. Kawai, and T. Kojima, *Jpn. J. Appl. Phys.* **23**, L657 (1984).
- <sup>12</sup> F. Bonell and S. Andrieu, *Surf. Sci.* **656**, 140 (2017).
- <sup>13</sup> N. Motegi, *J. Vac. Sci. Technol. B Microelectron. Nanom. Struct.* **13**, 1906 (1995).
- <sup>14</sup> T. Shima, K. Takanashi, Y. K. Takahashi, and K. Hono, *Appl. Phys. Lett.* **88**, 063117 (2006).
- <sup>15</sup> T. Niizeki, Y. Utsumi, R. Aoyama, H. Yanagihara, J. I. Inoue, Y. Yamasaki, H. Nakao, K. Koike, and E. Kita, *Appl. Phys. Lett.* **103**, 162407 (2013).
- <sup>16</sup> H. Yanagihara, M. Myoka, D. Isaka, T. Niizeki, K. Mibu, and E. Kita, *J. Phys. D: Appl. Phys.* **47**, 129501 (2014).
- <sup>17</sup> D. Reisinger, B. Blass, J. Klein, J. B. Philipp, M. Schonecke, A. Erb, L. Alff, and R. Gross, *Appl. Phys. A Mater. Sci. Process.* **77**, 619 (2003).
- <sup>18</sup> F. C. Voegt, T. Fujii, P. J. M. Smulders, L. Niesen, M. A. James, and T. Hibma, *Phys. Rev. B* **60**, 11193 (1999).
- <sup>19</sup> D. L. Schulz and G. J. McCarthy, *Powder Diffr.* **3**, 104 (1988).
- <sup>20</sup> A. Okamura, S. Nakamura, M. Tanaka, and K. Siratori, *J. Phys. Soc. Japan* **64**, 3484 (1995).
- <sup>21</sup> S. Chikazumi, *Physics of Ferromagnetism* (Wiley, 1964).